10 Gb/s single-mode vertical-cavity surface-emitting laser with large aperture and oxygen implantation

2004 Semicond. Sci. Technol. 19 L86

(http://iopscience.iop.org/0268-1242/19/8/L02)

INSTITUTE OF PHYSICS PUBLISHING SEMICONDUCTOR SCIENCE AND TECHNOLOGY
Semicond. Sci. Technol. **19** (2004) L86–L89 PII: S0268-1242(04)79330-X

LETTER TO THE EDITOR

10 Gb/s single-mode vertical-cavity surface-emitting laser with large aperture and oxygen implantation

Fang-I Lai[1], Tao-Hung Hsueh[1], Ya-Hsien Chang[1], Hao-Chung Kuo[1], S C Wang[1], Li-Hong Laih[2], C P Song[3] and H P Yang[3]

[1] Institute of Electro-optical Engineering, National Chiao-Tung University, Hsin-Chu, Taiwan, Republic of China
[2] Millennium Communication Co., Ltd, Hsinchu Industrial Park, Hsinchu Hsien, Taiwan
[3] Opto-Electronics & Systems Laboratories of the Industrial Technology Research Institute, Hsin-Chu, Taiwan, Republic of China

E-mail: hckuo@faculty.nctu.edu.tw

Received 20 April 2004
Published 21 June 2004
Online at stacks.iop.org/SST/19/L86
doi:10.1088/0268-1242/19/8/L02

Abstract
High-speed single transverse mode 850 nm vertical cavity surface emitting lasers (VCSELs) with large emission aperture with a diameter of 8 μm were fabricated. These VCSELs exhibit good performance with threshold currents of 1.5 mA, a single transverse mode emission within the full operational range and a maximum output power of 3.8 mW. The large aperture is advantageous to these VCSELs with a smaller dynamic resistance (60 Ω) than that of conventional single-mode VCSEL. These single-mode VCSELs also demonstrate superior high-speed performance up to 10 Gb s^{-1}.

(Some figures in this article are in colour only in the electronic version)

1. Introduction

Vertical cavity surface emitting lasers (VCSELs) have become a standard applied technology in local area networks (LANs) from 1.25 Gb s^{-1} to 10 Gb s^{-1}. The main advantages of VCSELs are their low threshold current, low divergent angle and circular beam, which simplify packaging and reduce electrical power consumption. The surface emission from the VCSELs also facilitates the integration of a two-dimensional array and the testing of wafer levels, reducing the cost of fabrication [1]. High-power single transverse mode operation is preferred for many applications, including laser printing, optical storage and long-wavelength telecommunications. Two major approaches were previously developed for fabricating single-mode VCSELs. The first is to make the current-confined aperture sufficiently small to support only the fundamental mode; the best results using this method have been achieved using oxide-confined VCSELs [2]. Typically, the current-confined aperture must be less than 3 μm in diameter to ensure stable single-mode operation. However, the large resistance inherited from the small aperture limits the modulation bandwidth and degrades the high-speed performance. Furthermore, the lifetime of the oxide VCSEL decreases proportionally as the diameter of the oxide aperture declines, even when the device is operated at a reduced current [3].

The second approach for fabricating a single-mode VCSEL is to suppress the high-order mode in a multimode VCSEL by surface-relief etching [4, 5], or by extending the optical cavity [6]. Young *et al* proposed hybrid implant/oxide VCSELs that support single-mode operation, based on 'cold-cavity' considerations. The basic concept is to increase the optical losses of higher order modes [7]. However, the threshold current (I_{th}) of this VCSEL is rather high, at

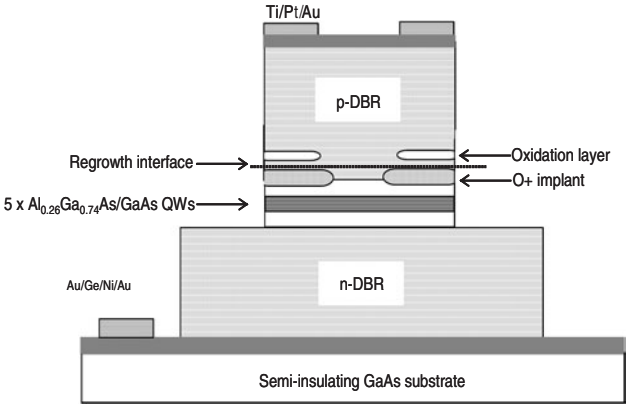

Figure 1. The schematic structure of a single-mode VCSEL. The O^+-implanted aperture is 8 μm in diameter and the oxidation aperture is 10 μm in diameter.

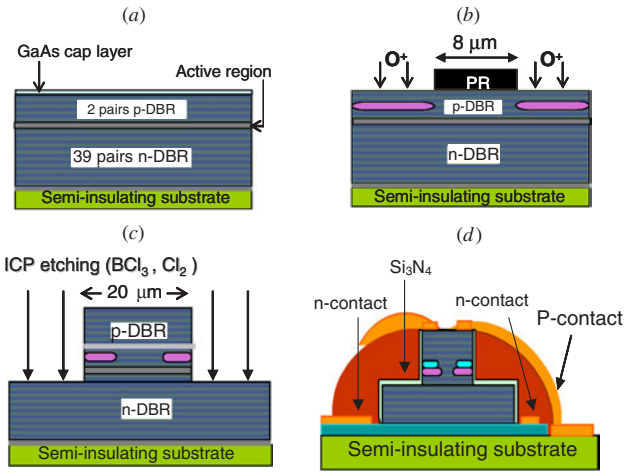

Figure 2. Device process flowchart. (*a*) The VCSEL with 39 pairs of n-type DBRs, 5-QW, two pairs of p-type DBRs and a 50 Å GaAs cap layer. (*b*) The O^+-implanted aperture was defined by photolithography. (*c*) The surface relief pattern with a diameter of 20 μm was etched by chemically assisted RIE (reactive ion etching). (*d*) Ti/Au were deposited for metal interconnects and coplanar waveguide probe-bond pads.

~5.8 mA. This study presents a low I_{th}, high-power single-mode VCSEL fabricated using oxygen (O^+) implantation, MOCVD regrowth and selective oxidation. Two types of apertures in this device were designed to reduce the overlap of the higher order modes with the current-confined profile while at the same time keeping a sufficient fundamental mode/current-confined overlap [8]. The current flow is confined by an oxygen-implanted aperture with a diameter of 8 μm and the optical mode is confined by an oxide aperture with a diameter of 10 μm. These VCSELs emit a single transverse mode within the full range of the operated current and can operate up to 10 Gb s^{-1}.

2. Device structure and fabrication

Figure 1 schematically depicts the cross-sectional O^+-implanted VCSEL structure. The epitaxial structure was grown by metal organic chemical vapour deposition (MOCVD) on a semi-insulated GaAs (100) at 6° to (111A) substrate. Prior to O^+ implantation, the wafer structure consists of an n^+-GaAs (Si-doped) buffer layer and 39 pairs of n-type (Si-doped) $Al_{0.19}Ga_{0.81}As/Al_{0.9}Ga_{0.1}As$ bottom-distributed Bragg reflectors (DBRs), an $Al_{0.26}Ga_{0.74}As/GaAs$ five period quantum-well (QW) active region in a one-wavelength cavity for 850 nm emission and two pairs of p-type (C-doped) $Al_{0.19}Ga_{0.81}As/Al_{0.9}Ga_{0.1}As$ top-DBRs. Then, a 50 Å GaAs cap layer was grown at the null position of the optical field to avoid optical absorption; the GaAs layer was used to prevent oxidation of the surface before regrowth. O^+ was implanted (dosage ~2×10^{14}) at 120 keV to define a current aperture with a diameter of 8 μm by photolithography, as indicated in figures 2(*a*) and (*b*). After implantation, 24 pairs of top-DBRs were regrown with a 30 nm $Al_{0.98}Ga_{0.02}As$ oxide layer which is located at the third null node position. This position is one pair away from the QW region, compared to conventional VCSELs, to reduce the index guiding effect. During the regrowth period, the implanted layer became an effective insulator as the current-confined aperture because of the activation process. The processing sequence included six photomasks to fabricate oxide-confined polyimide-planarized VCSELs with coplanar wave-guide probe pads. This process was designed to minimize capacitance while keeping reasonably low resistance. Device fabrication began with the formation of cylindrical mesas 20 μm in diameter by etching the surrounding semiconductor to a depth of 5 μm into the bottom n-type mirror using a reactive ion etching (RIE) system as shown in figure 2(*c*). The gas used in the ion source was Cl_2, and the gas that flowed on the sample was BCl_3. The samples were then selectively oxidized to form circular optical confined apertures with a diameter of 10 μm. Following this Si_3N_4 was deposited for passivation. Ti/Au was evaporated for the p-type contact ring, and AuGeNi/Au was evaporated onto the etched n-buffer layer etched bottom mirror to form the n-type contact which is connected to the semi-insulating substrate. Contacts were alloyed for 30 s at 420 °C using RTA. After contact formation, photosensitive polyimide was spun on the sample for field insulation and planarization. Ti/Au with thicknesses of 200/3000 Å were deposited for metal interconnects and coplanar waveguide probe-bond pads (figure 2(*d*)). Heat treatment after the metal deposition was utilized to improve metal-to-polyimide adhesion strength. For comparison, a conventional VCSEL was also processed with only an oxide-confined aperture with a diameter of 8 μm. The same processes as above were performed but without O^+ implantation and regrowth process.

3. Results and discussion

Figure 3(*a*) plots the continuous-wave (CW) power–current–voltage (L–I–V) curves and the spectral characteristics (insertion) of the O^+-implanted VCSELs. The VCSEL emits near 3.8 mW peak power at a 12.3 mA drive current and exhibits a low threshold current of 1.5 mA with a threshold voltage of 1.7 V and slope efficiencies of ~ 0.35 W A^{-1}. The insets of figure 3(*a*) present the emission spectrum and the near-field pattern of the device at 10 mA. The figure reveals that only the fundamental mode is present over the full range of operational current. Over 90% of the series resistances

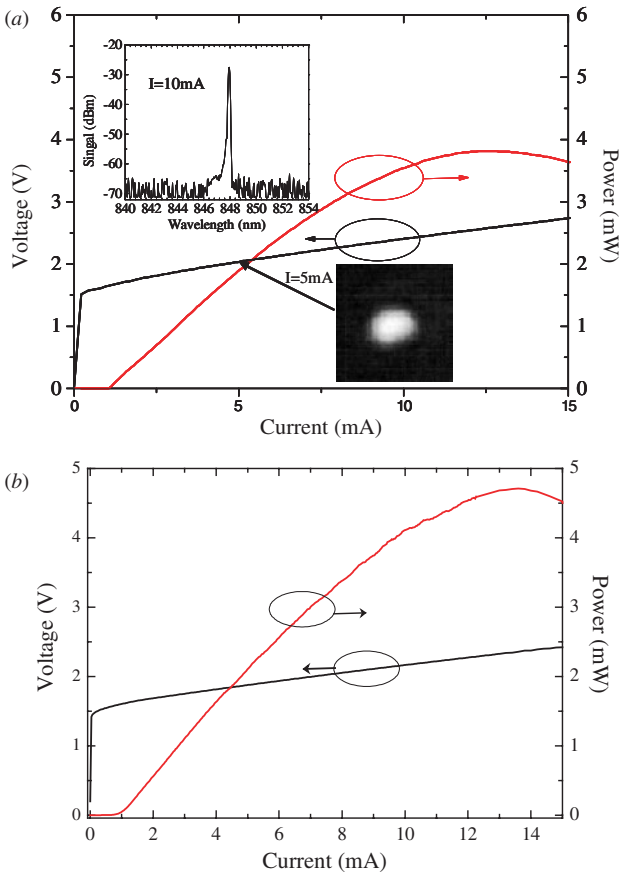

Figure 3. (*a*) L–I–V curves, spectral characteristics and the near-field pattern of the O^+-implanted VCSEL. The emission spectrum is obtained at 10 mA and the near-field pattern is obtained at 5 mA. They demonstrate that the O^+-implanted VCSEL has a fundamental mode only over the full operating range. (*b*) L–I–V curves of the comparable conventional VCSEL.

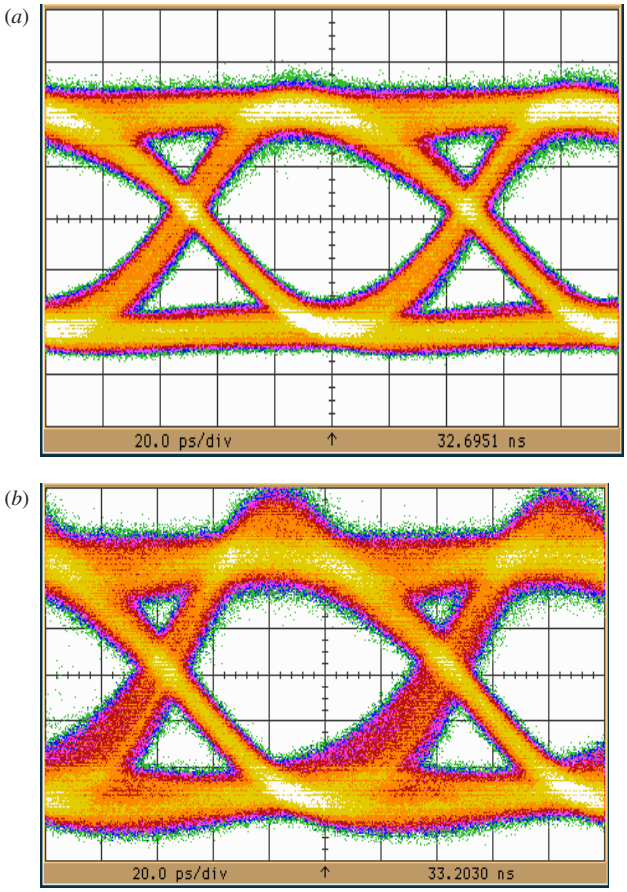

Figure 4. Characteristic eye diagram of (*a*) large-aperture single-mode VCSEL with a diameter of 8 μm; (*b*) conventional multi-mode VCSELs with a diameter of 8 μm, transmitted at 10 Gb s^{-1} with a bias of 5 mA and an extinct ratio of 6 dB.

of the VCSELs are 60–65 Ω. This range of resistance is almost the same as that for comparable conventional VCSELs (the L–I–V characteristics are shown in figure 3(*b*)), but lower than for single-mode VCSELs with a small aperture, which typically have around 250 Ω of series resistance [9]. Additionally, the roll-over current is about 12 mA, which exceeds that of the single-mode VCSEL with a small aperture and so the proposed VCSELs should be more reliable [2]. Figure 3(*b*) plots the L–I–V characteristics of the comparable conventional VCSEL. The threshold current (I_{th}) of the VCSEL is around 1 mA with a threshold voltage of 1.5 V and the slope efficiency of ∼0.4 W A^{-1}. The peak output power is 4.7 mW at a drive current of 12.3 mA. Although the O^+-implanted VCSELs have a lower peak power and a higher I_{th} than comparable conventional VCSELs, perhaps because of the regrowth interface and the losses of higher order modes, the O^+-implanted VCSELs can operate in the fundamental single mode within the full operating range exhibiting a better high-speed modulation response than conventional VCSELs [10].

To measure the high-speed characteristic of the O^+-implanted and comparable conventional VCSELs under large signal modulation, microwave and light wave probes were used in conjunction with a 10 Gb s^{-1} ($2^{23} - 1$ long pseudorandom bit sequence generated) pattern generator (MP1763 Anritsu). A 12.5 GHz New Focus photoreceiver with an OC-192 low pass Bessel Thompson filter was used for detection. The eye diagrams were obtained for back-to-back (BTB) transmission of VCSELs. Figures 4(*a*) and 4(*b*) demonstrate the eye patterns of O^+-implanted and comparable conventional VCSELs, respectively. Figure 4(*a*) shows the wide-open eye pattern, indicating good performance of the O^+-implanted single-mode VCSEL. The rise time (T_r) and the fall time (T_f) are estimated to be 28 ps and 38 ps, respectively, with jitter (p–p) = 14 ps. The comparable conventional oxide-confined multiple-mode VCSEL yields a more noisy eye pattern, with jitter = 17 ps (see figure 4(*b*)).

4. Summary

This study reports a new technique for fabricating a single-mode VCSEL with a large emission aperture with a diameter of 8 μm, using oxygen implantation, MOCVD regrowth and selective oxidation. The single-mode VCSELs have a low I_{th} of about 1.5 mA and a high output power of 3.8 mW. Although this approach involves regrowth, it provides the single transverse mode with large aperture with a low I_{th} and a high output power. These single-mode VCSELs also demonstrate superior high-speed performance up to 10 Gb s^{-1}. The authors believe that the concept can be applied to fabricate long-wavelength single-mode VCSELs.

Acknowledgments

The authors would like to thank Drs C P Kuo of LuxNet Corporation, and Professor S L Chuang of University of Illinois for useful discussions and technical support. This work was partially supported by the National Science Council of the Republic of China (ROC) in Taiwan under contract no NSC 90-2215-E-009-102 and by the Academic Excellence Program of the ROC Ministry of Education under contract no 88-FA06-AB. The support by the Institute of Nuclear Energy under contract no 922001InER015 of the proton implantation is also gratefully acknowledged.

References

[1] Choquette K D and Geib K M 1999 Fabrication and performance of vertical cavity surface-emitting lasers *Vertical-Cavity Surface-EmittingLasers* ed C Wilmsen, H Temkin and L Coldren (Cambridge: Cambridge University Press) chapter 5

[2] Jung C, Jager R, Grabherr M, Schnitzer P, Michalzik R, Weigl B, Muller S and Ebeling K J 1997 *Electron. Lett.* **33** 1790–1

[3] Hawkins B M, Hawthorne R A III, Guenter J K, Tatum J A and Biard J R 2002 *ECTC 2002*

[4] Martinsson H, Vukusic J A, Grabherr M, Michalzik R, Jager R, Ebeling K J and Larsson A 1999 *IEEE Photon. Technol. Lett.* **11** 1536–8

[5] Wiedenmann D, King R, Jung C, Jäger R, Schnitzer P, Michalzik R and Ebeling K J 1999 *IEEE J. Quantum Electron.* **5** 503–11

[6] Unold H J, Mahmoud S W Z, Jager R, Kicherer M, Riedl M C and Ebeling K J 2000 *IEEE Photon. Technol. Lett.* **12** 939–41

[7] Young E W, Choquette K D, Chuang S L, Geib K M, Fischer A J and Allerman A A 2001 *IEEE Photon. Technol. Lett.* **13** 927–9

[8] Seurin Jean-Francois P, Chuang Shun Lien, Chirovsky Leo M F and Choquette K D 2002 *Laser Focus World* **38**

[9] Yokouchi N, Iwai N and Kasukawa A 2003 Presented at *Photonic West 2003* vol 4994 pp 189–96

[10] Haglund Å, Gustavsson J S, Vukusic J, Modh P and Larsson A 2004 *IEEE Photon. Technol. Lett.* **16** 368–70